

## Model based detection of hydrogen leaks in a fuel cell stack

Ari Ingimundarson and Anna G. Stefanopoulou and Denise McKay

**Abstract**—Hydrogen leaks are potentially dangerous faults in fuel cell systems. The paper presents an approach to detect hydrogen leaks. The method is applicable during startup and shutdown as well as normal operating conditions. The method relies on simple mass balance equations but takes into account the natural leak of the stack and humidity. Hydrogen leak detection without using relative humidity sensors is specially studied. In that case, adaptive alarm thresholds are given so that false alarms due to the lack of humidity sensors are eliminated. The validity of the method is also discussed in terms of common hydrogen supply system configurations. The detection method is validated on an real fuel cell laboratory rig where leaks could be introduced in a controlled manner.

Fuel cells, fault detection, leak detection, hydrogen leakage.

### I. INTRODUCTION

A common safety concern for fuel cell systems are hydrogen leaks. As hydrogen is a combustible material its uncontrolled release can carry risks. In [1] the safety characteristics of hydrogen compared to other common fuels are presented. This paper shows how hydrogen leaks on the anode side of a fuel cell can be detected using sensors commonly used for control in addition to a flow meter in a pure hydrogen polymer electrolyte membrane (PEM) fuel cell stack.

Hydrogen has the lowest molecular weight and viscosity of any gas. Due to its properties it has a faster leak rate through small orifices than all other gases, see [2]. It is difficult to contain hydrogen gas as it escapes easily. In pure hydrogen fuel cell stacks there is always an accepted leak level as it is impossible to completely seal the cells. An increase in leak due to rupture of seals can be the cause of a critical concentration of  $H_2$  to form which in turn can lead to an explosion.

The standard solution to hydrogen leak detection is to install hydrogen sensors at strategically selected places close to the fuel cell stack and/or submit the system to periodic inspections. The sensors are expensive so other ways of leak detection are of interest.

Leak detection of gases has been studied by [3] as a part of a diagnosis system for the air path of an automotive diesel engine. There the pressure is similar to what can be expected on the anode and cathode side of a PEM fuel cell or from 100 – 200 kPa. An important difference between the problems is that an estimation of the hydrogen leak has to take into account the presence of vapor in the anode. Vapor

pressure in the anode can vary spatially in the stack as the hydrogen often enters dry while at the outlet of the anode the vapor might be at saturation pressure. The vapor pressure can also change significantly during operation, specially when the anode is purged periodically. Purging of the anode gases is a frequent solution to get rid of excess liquid water and inert gas blankets from the membrane, see [4]. As the total gas leak is assumed to depend on the pressure difference between the anode and the surroundings the hydrogen leak will depend on the composition of the gas where the leak takes place.

Two approaches are presented here to address this problem, one based on decoupling the effect by measuring vapor pressure directly with relative humidity sensors. The other is to use the fact that vapor pressure is limited above by the saturation pressure. This can be used to create an adaptive alarm thresholds.

A lot of current research in fuel cells has the goal to eliminate the need to humidify the entering gases. But as the fuel cell produces water and due to the back diffusion through the membrane, vapor will always be present in the anode. This becomes specially important as membranes become thinner because vapor back diffusion increases when membranes are thinner.

The presented work also has many similarities to [5] where an observer was designed to estimate hydrogen pressure in the anode. The observer there contains an output-injection term based on stack voltage. In [6] additional flow and pressure measurements are used to estimate the partial pressure of hydrogen as there are very many phenomena that can affect stack voltage besides hydrogen pressure.

In this paper, two leakage test quantities are presented and compared for advantages and disadvantages. A test quantity is simply a scalar value calculated from process data that is supposed to refute validity of assumptions associated with it. The test quantity is refuted if it rises above a predetermined threshold. The main assumption that the presented test quantity is supposed to refute in the current article is that no leak is present, see [7]. Exact interpretation of the test quantities will be presented in Section III. Test quantities are referred to as Analytical Redundancy Relations (ARR) in the fault detection literature.

The main requirements for the leakage detection is swift and reliable detection along with simplicity in evaluation. The fewer sensors the detection method depends on, the better it is as sensor faults can be interpreted as leaks. This justifies further the attention on hydrogen leak detection without using relative humidity sensors.

A crucial sensor for the presented method is the hydrogen

A. Ingimundarson is with the Automatic Control Department, Campus de Terrassa, Technical University of Catalonia, Rambla Sant Nebridi, 10, 08222 Terrassa, Spain, e-mail: {ari.ingimundarson}@upc.edu

A. G. Stefanopoulou and D. McKay are with the Fuel Cell Control Laboratory, Mechanical Engineering, University of Michigan, 1231 Beal Avenue Ann Arbor, MI, 48109, {annastef, dmckay}@umich.edu

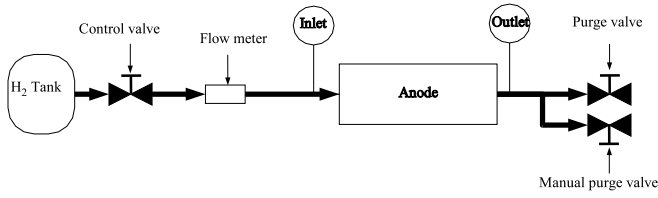


Fig. 1. The configuration of the hydrogen supply system.

flow meter. Often such meters are not present in fuel cell configurations. The most common solution to control the amount of hydrogen in the anode is to control the pressure in the anode with a pressure control valve. On the other hand, a hydrogen flow meter might be used for other failure detection algorithms and also for fuel economy calculations. A hydrogen flow meter based on hot wire anemometry was present in the fuel cell laboratory rig on which the method was tested.

In Section II the model of the fuel supply subsystem is presented. In Section III the test quantities are introduced. In Section IV the test quantities are validated on data from a laboratory rig. In Section V an adaptive threshold is introduced when no relative humidity sensor is present. Section VI discusses the validity of the test quantities for common hydrogen supply system configurations. Finally in Section VII some conclusions are drawn.

## II. MODEL OF THE FUEL SUPPLY SYSTEM

The fuel supply subsystem supplies hydrogen gas at the desired pressure to the fuel cell stack. The gas from the high pressure cylinder is depressurized through a series of control valves to a pressure similar to the air on the cathode side.

The stack used for this investigation has 24 PEM fuel cells with 300 cm<sup>2</sup> active surface area of GORE<sup>TM</sup> membrane electrode assemblies (MEAs) and Etek<sup>TM</sup> gas diffusion layers. The stack was designed and assembled in the Schatz Energy Research Center at Humboldt State University for the Fuel Cell Control Laboratory at the University of Michigan. The stack is water cooled and contains an internal humidification section that diffuses water vapor after the power section coolant loop to the incoming air. The incoming hydrogen inlet gas is not externally humidified.

The stack can produce 1.25 kW continuous power at less than 400 mA/cm<sup>2</sup>. It is designed for operation at low temperatures (<70 C), and low gauge pressures (<12 kPa in cathode and 14–34 kPa in the anode).

A model of the breathing system of a PEM stack, based on similar model principles, was presented in [8]. High power density requirements suggest operating pressures and temperatures of PEM fuel cells up to  $2.7 \cdot 10^5$  Pa and 80°C. It should be noted that the fuel cell presented here has a larger natural leak area than fuel cell stacks not designed for laboratory experiments.

In Fig. 1 a schematic diagram of the main components are shown. The model is based on mass conservation of hydrogen in the anode. The anode is lumped into one control volume for which entering and exiting hydrogen mass flows

are calculated. Assuming that the hydrogen behaves as an ideal gas, the pressure in the anode is used to calculate the mass of hydrogen. The model presented is valid during startup and shutdown operating conditions. During startup and shutdown the pressure and temperature can be close to ambient conditions.

It is important when designing failure detection algorithms to be aware of the physical components that the model equations represent. The reason for this is that failures are most often related to physical components. Notice that only the components relevant to leaks are shown in the schematic diagram in Fig. 1. Sensors of pressure, temperature and relative humidity were placed at the inlet and outlet of the anode volume. Sensors are placed at the inlet and outlet because variables can vary spatially along the flow channel. A common approximation is to assume that the variables change linearly between the inlet and outlet of the stack. Lumped variables were calculated as the average between inlet and outlet measurements of that variable.

### A. Nomenclature

The following symbols appear in the model equations presented in this paper. Mass is denoted by  $m$  in [kg], mass flow by  $Q$  in [kg/sec], pressure by  $p$  in [Pa], temperature by  $\theta$  in [K], volume by  $V$  in [m<sup>3</sup>], relative humidity by  $\phi$  on the scale 0 – 1, and molar mass of element  $i$  by  $M_i$ . The subscript  $H_2$  denotes hydrogen,  $v$  for vapor while an and atm stand for anode and atmosphere respectively.

### B. Model equations

The equations when no fault is present are

$$\frac{dm_{H_2}}{dt} = Q_{H_2,in} - M_{H_2} \frac{nI_{st}}{2F} - Q_{H_2,nl} \quad (1)$$

$$p_{an} = p_{H_2,an} + p_{v,an} \quad (2)$$

$$p_{,an} = \phi_{an} p_{sat}(\theta_{an}) \quad (3)$$

Assuming perfect mixing of gases within the control volume the mass flow of hydrogen  $Q_{H_2,nl}$ , due to the natural leak  $Q_{nl}$ , is calculated as

$$Q_{H_2,nl} = \frac{m_{H_2}}{m_{H_2} + m_w} Q_{nl} \quad (4)$$

$$= x_{H_2} Q_{nl} \quad (5)$$

where  $x_{H_2}$  is the mass fraction of hydrogen in the anode. The mass fraction is estimated using the following equation.

$$\begin{aligned} x_{H_2} &= \frac{p_{H_2,an}}{p_{H_2,an} + \frac{M_w}{M_{H_2}} p_{w,an}} \\ &= \frac{p_{an} - \phi_{an} p_{sat}(\theta_{an})}{p_{an} - \phi_{an} p_{sat}(\theta_{an}) + \frac{M_w}{M_{H_2}} \phi_{an} p_{sat}(\theta_{an})} \end{aligned} \quad (6)$$

The term  $Q_{nl}$  represents the natural leak from the anode of the fuel cell stack. This is the leak that is present from the beginning due to the fact that it is very difficult to seal 100% the electrodes of the stack. It is assumed that it is governed by a standard orifice relation given by Eq. (7). The effective

natural leak area,  $A_{nl}$  is specific for each stack so it has to be estimated before using the model.

$$Q_{nl} = \frac{A_{nl} p_{an}}{\sqrt{R \theta_{an}}} (p_r)^{1/\gamma} \left( \frac{2\gamma}{\gamma-1} \left[ 1 - (p_r)^{(\gamma-1)/\gamma} \right] \right)^{\frac{1}{2}} \quad (7)$$

$$= A_{nl} \psi \quad (8)$$

$$= Q_{H_2, nl} + Q_{v, nl} \quad (9)$$

where  $p_r = p_{an}/p_{atm}$ . For the anode control volume, relation (1) represents a simple mass conservation relation. As the mass of hydrogen can not be measured, it has to be estimated through the pressure with equation (2). For this estimation it is assumed that both hydrogen and vapor follow the ideal gas law. The vapor pressure can on the other hand also be estimated by measuring the relative humidity and temperature, see Eq. (3).

In Fig. 1 two purge valves are shown connected to the outlet of the anode control volume. It is common that excess water and inert gas blankets that diffuse from the cathode through the membrane are purged out of the anode by periodically opening a valve causing a large but temporary increase in flow rate of hydrogen through the flow channel on the anode side, see [4]. As the purge valve is electronically controlled, the fault detection algorithms can be disabled during purging so that the increased flow does not cause a false alarm. The laboratory rig on which tests were made also had a manual purge valve where leaks could be initiated in a controlled manner to test algorithms.

It is assumed that a hydrogen leak can be expressed as an increase in the leak area. If the leak area increases by  $\Delta A$ , this causes a flow increase

$$Q_{fault} = x_{H_2} \Delta A \psi. \quad (10)$$

### III. TEST QUANTITIES

A frequent choice of test quantities for a set of model relations are model validation measures. A common way to do this is to use a measurement and a model prediction of that measurement and form a quantity that expresses the distance between the two. The test quantity is large if the model is refuted but zero otherwise.

#### A. Test quantity 1. Parity equation based on anode pressure

The first test quantity is formed by substituting  $p_{H_2}$  in Eq. (2) with its equivalent using the ideal gas law,  $p_{H_2} = R_{H_2} m_{H_2} \theta_{an} / V_{an}$ . Taking the time derivative on both sides yields

$$\frac{dp_{an}}{dt} = \frac{dm_{H_2}}{dt} \frac{\theta_{an} R_{H_2}}{V_{an}} + \frac{d\theta_{an}}{dt} \frac{m_{H_2} R_{H_2}}{V_{an}} + \frac{dp_{w, an}}{dt}$$

The resulting time derivatives of vapor pressure and temperature are eliminated as they usually can safely be assumed to be much smaller than the other terms. When humidity of hydrogen entering the stack is actively controlled, for example by steam injection, this assumption should be verified carefully. Solving for the mass derivative and moving all terms to the right side of the equation one obtains as a test quantity

$$T_1(t) = \frac{dm_{H_2}}{dt} - \frac{V_{an}}{\theta_{an} R_{H_2}} \frac{dp_{an}}{dt} \quad (11)$$

which should be 0 when there is no extra leak in the fuel cell stack. Finally, the time derivative of  $m_{H_2}$  is replaced by expression (1). Notice that the leak term given by Eq. (10) affects directly  $T_1$ , i.e.,  $T_1 = Q_{fault}$ . Therefore  $T_1$  is actually an estimate of the increase in hydrogen leakage given with units [kg/sec].

The numerical derivative is implemented as suggested in [9] with a first-order low pass filter. The sampling time of all the measurements was 0.5 sec. The filter time constant was chosen as 2 sec. The hydrogen flow meter was supposed to have a 2 second time delay so that signal was not filtered.

#### B. Test quantity 2. Identification of change in leak area.

A common approach to failure detection of a process is to identify its parameters and see if they stay on a prescribed interval. If the parameter leaves the interval, a fault has occurred, see [10]. The second test quantity is based on this approach. An estimate is created of the change in the leak area,  $\Delta A_1$  from the natural leak  $A_{nl}$ . See [11] for a reference where a similar approach was presented.

One of the main advantages of this test quantity is that it returns a quantification of the increase in leak area. If, during operation, the fuel cell is subjected to large pressure differences, a certain increase in leak area detected at low pressure could avoid dangerous situations at higher pressures when a larger flow area would lead to a larger hydrogen flow.

Using the fact that the leak term given by Eq. (10) affects  $T_1$  directly, the second test quantity is formed as an estimate of  $\Delta A$

$$T_2(t) = \frac{T_1(t)}{x_{H_2} \psi} \quad (12)$$

$$= \Delta A \quad (13)$$

Eq. (12) is the evaluation equation of this test quantity while Eq. (13) shows how a leakage affects the test quantity.

When the pressure in the anode approaches atmospheric pressure, the term  $\psi$  approaches zero. This means that the estimate for  $\Delta A$  is not trustworthy. This test quantity might therefore have limited validity, specially at startup and shutdown when pressure in anode is close to atmospheric pressure.

#### C. Interpretation of test quantities

Related to each test quantity is a set of components on which the equations are based. Following the framework presented in [12] it is assumed that if all components are functioning normally the test quantities will not deviate from an interval around zero. These intervals correspond to lower and upper thresholds for the test quantities. The size of the intervals are determined from noise and model uncertainty, see Section IV. If the test quantity rises above the upper limit, it is assumed that at least one of the components is not functioning normally. A possible failure in this case is an increase in leak area which results in an increase in hydrogen leakage. If a test quantity drops below its threshold, at least one of the components is not functioning normally but an increase in leak area is excluded from the list of

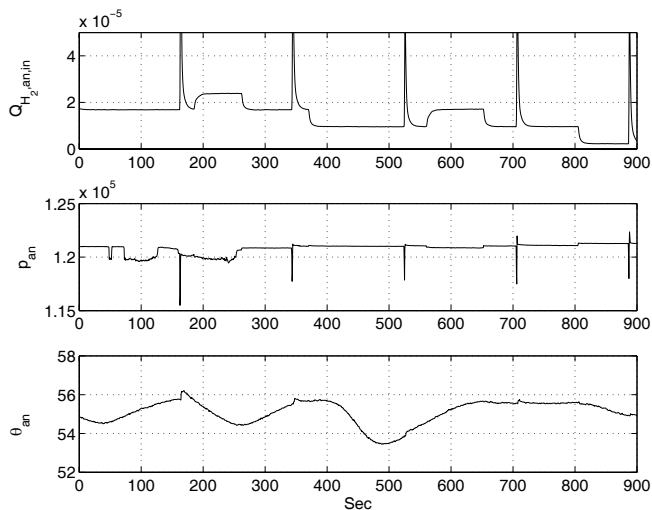


Fig. 2. Hydrogen mass flow,  $Q_{H_2,an,in}$  [kg/sec], anode pressure,  $p_{an}$  [Pa] and anode temperature,  $T_{an}$  [ $^{\circ}C$ ] for the data series considered.

possible faults as the fault parameter  $\Delta A$  affects each test quantity positively. Notice that it is not assumed that if the test quantities are inside of their intervals, all components are functioning normally. The test quantities serve only to invalidate assumptions related to them.

As there are a number of components related to each test quantity, one can not directly assume that a hydrogen leak is present when a test quantity rises above the threshold without further information. In the context of the current article it is assumed that other faults have been considered less probable either with hardware redundancy or by probabilistic arguments about other components (failure rate of sensors) or by construction of other test quantities. From this argument it is clear that the fewer components that support a test quantity, the better.

#### IV. VALIDATION OF TEST QUANTITIES

The presented test quantities should all equal zero when no fault is present. Any discrepancy from zero is due to model errors and measurement noise. As these error sources will always be present it is vital to try the test quantities without fault over as many operating regions as possible to determine the interval that the test quantities stay on in the fault free case.

The test quantities were calculated for the experiment shown in Figs 2 and 3. The graph of the hydrogen flow requires further explanation. The spikes at times 162, 343, 524, 705 and 886 second in hydrogen flow are due to purging of hydrogen from the anode as mentioned in section II. The moderate rise at times 185 and 560 seconds are due to leaks that were provoked by opening the manual purge valve. Furthermore it should be noted that the variations in anode pressure at times 50-250 seconds occurred due to a fault in the anode pressure sensor. As the variation was small this has no effect on the calculation of the test quantities.

During this experiment, two values from the power range of the stack were tested. In the last part of the data series no

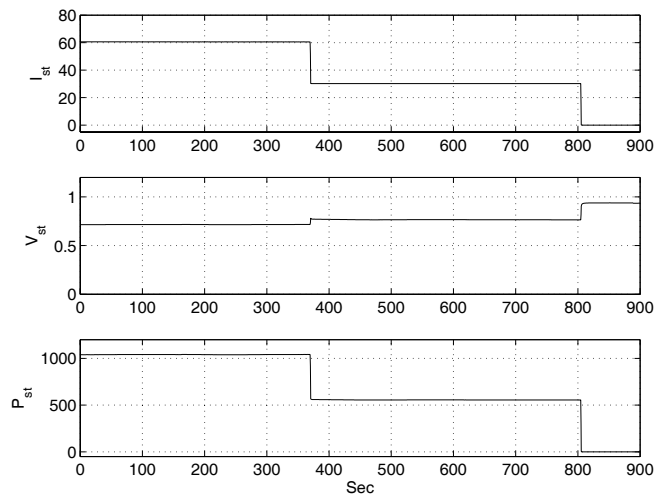


Fig. 3. Stack current,  $I_{st}$  [Amp], average cell voltage,  $V_{st}$  [Volt] and stack power,  $P_{st}$  [W] for the data series considered.

current is drawn from the stack. In this case the hydrogen flow corresponds to the natural leakage of the stack, which was estimated to be around  $Q_{nl} = 2 \cdot 10^{-6}$ .

In Fig. 4 the test quantities are shown for the data series. Notice that the scales of the test quantities are different by orders of magnitudes as they measure different physical quantities.  $T_1$  measures directly the leakage in [kg/sec] and can be compared to the actual hydrogen usage in Fig. 2. It can be seen in Fig. 4 that the test quantity rises to around  $6 \cdot 10^{-6}$  when the leak was provoked with the manual valve. This corresponds to around 3 times the natural leak.

$T_2$  on the other hand measures the increase in leak area. This graph can be compared to the natural leak  $A_{nl}$  which was calculated as  $1 \cdot 10^{-8}$ . The graph shows that  $\Delta A$  increases to about  $3 \cdot 10^{-8}$  when the leak occurs. Again this corresponds to around 3 times the natural leak area.

Notice that model uncertainty is apparent in the figure as the test quantities are not exactly equal to zero at any time. Test quantities  $T_1$  and  $T_2$  are negative at high power output. This is probably due to an overestimation of natural leak at these operating conditions. Notice also that all test quantities jump considerably when there is a change in power output. These jumps are on the other hand significantly smaller than the rise due to the provoked leaks which on the other hand were around 3 times the natural leak of the stack. This indicates that an increase in leak smaller than the natural leak should be distinguishable from model uncertainty and noise.

#### V. HYDROGEN LEAK DETECTION WITHOUT USING HUMIDITY SENSORS

Simplifications will be presented for the test quantities which aim at terminating dependence on the relative humidity sensors. Notice that the two test quantities presented depend on all components (sensors) discussed in Section II.

Omitting sensors causes errors in the test quantities as the previously measured variable is not known but has to be

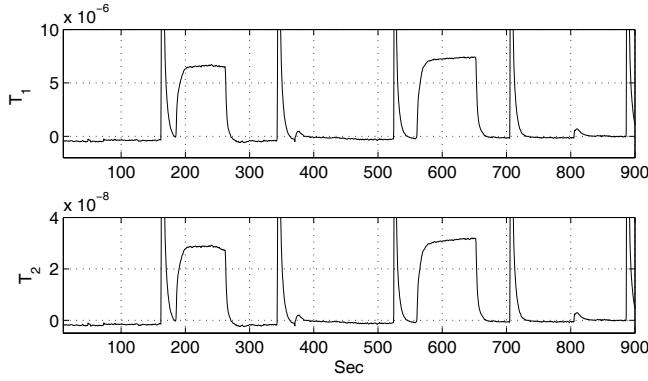


Fig. 4. Test quantities calculated for the data series.

estimated or replaced by a constant. Estimation of relative humidity was treated in [13]. For simplicity the approach taken here is to assume that relative humidity is constant.

Errors in the test quantities can cause false alarms or missed detections. To eliminate the risk of false alarms an adaptive alarm threshold is calculated so that if the test quantity rises above this threshold, it is guaranteed that the high value of the test quantity is not only due to the absence of the relative humidity sensors. Eliminating the risk of false alarms gives on the other hand rise to the possibility of missed detections. This is the situation when leaks occur and the associated test quantities does not rise above this new alarm threshold. Therefore, along with the new threshold the maximum leak that can go undetected is quantified.

The constant relative humidity which is used in the calculation of the test quantities is denoted  $\bar{\phi}$ . As the relative humidity only enters the test quantities through the calculation of the mass fraction in Eq. (6) the same notion is introduced for the  $x_{H_2}$ .  $\bar{x}_{H_2}$  is the mass fraction calculated with  $\bar{\phi}$ . The new alarm threshold is calculated by maximizing the possible error in  $T_1$  and  $T_2$  due to a difference between  $x_{H_2}$  and  $\bar{x}_{H_2}$ . Assume  $\bar{x}_{H_2}$  is used to calculate  $T_1$ . Adding and subtracting  $x_{H_2}$  from this equation and using the fact that  $T_1$  equals zero when  $\Delta A$  is zero, the following expression is obtained for the error due to replacing  $x_{H_2}$  with  $\bar{x}_{H_2}$ .

$$\Delta T_1 = -A_{nl}(\bar{x}_{H_2} - x_{H_2})\psi \quad (14)$$

In the case of  $T_2$  the error is

$$\Delta T_2 = -A_{nl} \frac{\bar{x}_{H_2} - x_{H_2}}{\bar{x}_{H_2}} \quad (15)$$

The new alarm threshold is obtained by maximizing  $\Delta T_1$  and  $\Delta T_2$ . It is obvious that this corresponds to minimizing  $\bar{x}_{H_2}$  and maximizing  $x_{H_2}$  over the range of possible values of  $\phi$ .  $\phi$  is physically limited to the range  $[0, 1]$ . When only these limits are considered, minimizing  $\bar{x}_{H_2}$  corresponds to choosing  $\bar{\phi} = 1$ , that is, it is assumed that the anode is fully humidified. The largest possible value of  $x_{H_2}$  is one, corresponding to the case when the anode contains no vapor. If extra information is available about the range of  $\phi$  this can be used to make the threshold less conservative. Generally,

the maximum value of  $\phi$  is used to calculate  $\bar{x}_{H_2}$  while the minimum is used to calculate  $x_{H_2}$ .

The maximum values of  $\Delta T_1$  and  $\Delta T_2$  correspond to the case when it is assumed that anode has the highest possible relative humidity while actually it is at its minimum. With relative humidity at its minimum, the gas that escapes through the natural leak area has a higher hydrogen content which in turn causes the need for more hydrogen to enter the anode. The rise in hydrogen flow then causes the test quantities to rise.

In Fig. 5 the adaptive thresholds given by Eqs. (14) and (15) are shown for the two test quantities. Two values of  $\phi$  are considered. In the first it is assumed that the hydrogen can be dry in the anode (to calculate  $x_{H_2}$ ,  $\phi = 0$  is used) while in the other it is assumed that the relative humidity will never drop below 50% ( $\phi = 0.5$ ). It is seen that in one case the leaks are not detected while in the other they are.

A number of comments are in order at this point. The adaptive thresholds depend on three things principally, natural leak of the stack,  $A_{nl}$ , anode pressure,  $p_{an}$  and anode temperature  $\theta_{an}$ . The dependance on  $A_{nl}$  means that if the stack is very tight to begin with, humidity sensors are not necessary as the adaptive threshold would be very small. This makes sense since if the stack is tight, the detection of leaks becomes strictly a matter of balancing the reacted hydrogen with the inflow into the anode. Humidity sensors can therefore be omitted if the stack has a small natural leak. The adaptive threshold also depends on pressure in the anode. The data presented here were taken for a stack that works on relatively low pressure (1.2 bar). Sometimes stacks are designed for high pressure (2 bar) to increase the power density. This would mean more hydrogen in the stack which in turn would mean a lower threshold. This on the other hand could be compensated by the fact that the operating temperature is often as high as 80 degrees. Higher temperature increases the saturation pressure, which in turn increases the adaptive threshold.

It was shown in Fig. 5 that leaks would have gone undetected using the upper adaptive threshold. Notice that it is easy to estimate the maximum undetected leak with the adaptive threshold compared to the natural leak by looking at Eqs. (14) and (15). As the adaptive threshold has units of hydrogen flow and increase in leak area it indicates directly what leak or increase in leak area could go undetected at each time.

## VI. CONFIGURATIONS OF FUEL SUPPLY SYSTEMS

In Fig. 6 common configurations of hydrogen supply systems for PEM fuel cell stacks are shown, see [4]. The main difference between these configurations and the one presented in Fig. 1 is the recirculation circuit that is used to increase the flow rate of hydrogen through the anode.

The applicability of the presented test quantities for these configurations would primarily depend on whether the recirculation circuit could accumulate hydrogen, i.e., temporarily more hydrogen would enter the circuit than leave it back to the anode. If the circuit could accumulate hydrogen, a false

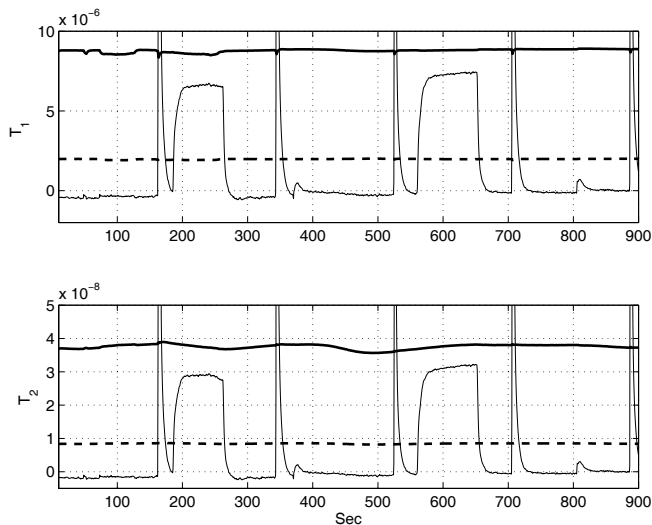


Fig. 5. Simplified test quantities (solid thin line) with adaptive alarm thresholds (solid thick line,  $\phi = 1$ ,  $\phi = 0$ , dashed thick line,  $\phi = 1$ ,  $\phi = 0.5$ )

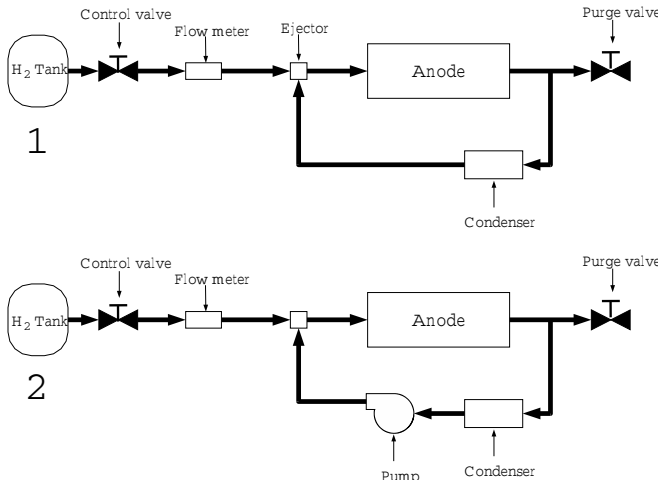


Fig. 6. Common configurations of hydrogen supply systems.

alarm could be sounded as the test quantities are based on mass balances of hydrogen.

Commonly the recirculation circuits do not have a large volume, nor are they operated at large pressures, both of which would be necessary for the circuit to accumulate hydrogen. Probably in most cases the test quantities could be used for hydrogen leak detection even when recirculation circuits are present in the hydrogen supply system.

In fuel cell stacks fed with reformed hydrocarbon fuel, such as natural gas, there is a high concentration of carbon dioxide and nitrogen in the anode that requires continuous flow out of the fuel cell anode. In this case, a model of the hydrogen flow out of the fuel cell anode is necessary. Moreover, there is a need for a good adaptive threshold to account for uncertainty in the anode inlet hydrogen composition. Future work will address these issues.

## VII. CONCLUSIONS

In this paper, model based hydrogen leak detection for PEM fuel cell systems has been considered. A model for the anode based on mass balances has been presented. The model was used to create two test quantities which were validated and compared using data from a fuel cell laboratory rig where leaks in the anode could be introduced in a controlled manner.

As the vapor pressure can vary inside the anode an adaptive threshold was presented for the test quantities so that false alarms could be avoided when information of vapor pressure is not available. The adaptive thresholds also serve to eliminate the dependence on relative humidity sensors for hydrogen leak detection. The dependence of this adaptive threshold on natural leak area, pressure and stack temperature was discussed. Finally the validity of the presented method when applied to common configurations of hydrogen supply systems was discussed and motivated.

## ACKNOWLEDGEMENTS

The authors acknowledge the support received from the Research Commission of the "Generalitat de Catalunya" (group SAC ref.2001/SGR/00236), the US National Science Foundation (NSF), and the Ford Motor Company.

## REFERENCES

- [1] J. Alcock, L. Shirvill, and R. Cracknell, "Compilation of existing safety data on hydrogen and comparative fuels," Shell Global Solutions, Tech. Rep., May 2001.
- [2] J. Larminie and A. Dicks, *Fuel Cell Systems Explained*. John Wiley & Sons, 2003.
- [3] M. T. S. Nyberg, "Model based diagnosis of the air path of an automotive diesel engine," *Control Engineering Practice*, vol. 12, pp. 513–525, 2004.
- [4] P. Rodatz, A. Tsukada, M. Mladek, and L. Guzzella, "Efficiency improvements by pulsed hydrogen supply in pem fuel cell systems," in *IFAC World Congress*, Barcelona, Spain, 2002.
- [5] M. Arcaç, H. Görgün, L. M. Pedersen, and S. Varigonda, "A nonlinear observer design for fuel cell hydrogen estimation," *IEEE Transaction on Control System Technology*, vol. 12, pp. 101–110, 2004.
- [6] J. Pukrushpan, A. Stefanopoulou, and H. Peng, "Control of natural gas catalytic partial oxidation for hydrogen generation in fuel cell applications," *IEEE Transactions on Control Systems Technology*, vol. 13, pp. 3–14, 2005.
- [7] M. Nyberg, "Model based fault diagnosis: Methods, theory, and automotive engine applications," Ph.D. dissertation, Linköpings Universitet, June 1999.
- [8] J. Pukrushpan, H. Peng, and A. Stefanopoulou, "Control-oriented modeling and analysis for automotive fuel cell system," *Journal of Dynamic Systems, Measurement, and Control*, vol. 126, pp. 14–25, 2004.
- [9] M. Kinnaert, "Fault diagnosis based on analytical models for linear and nonlinear systems - a tutorial," *Proceedings of IFAC Safeprocess'03*, pp. 37–50, 2003.
- [10] R. Isermann, "Process fault detection based on modeling and estimation methods—A survey," *Automatica*, vol. 20, pp. 387–404, 1984.
- [11] T. Höfling and R. Isermann, "Fault detection based on adaptive parity equations and single-parameter tracking," *Control Engineering Practice*, vol. 4, pp. 1361–1369, 1996.
- [12] M. Nyberg and M. Krysander, "Combining AI, FDI and statistical hypothesis-testing in a framework for diagnosis," *Proceedings of IFAC Safeprocess'03*, pp. 891–896, 2003.
- [13] D. McKay and A. Stefanopoulou, "Parametrization and validation of a lumped parameter diffusion model for fuel cell stack membrane humidity estimation," in *Proceedings of ACC*, 2004.